ON THE USE OF RIGID BODY MODES TO THE DEFLATED PRECONDITIONED CONJUGATE GRADIENT METHOD*

T.B. JÖNSTHÖVEL†, M.B. VAN GIJZEN, AND C. VUIK‡

1. Introduction

Finite element computations are indispensable for the simulation of material behavior. Recent developments in visualization and meshing software give rise to high-quality but very large meshes. As a result, large systems with millions of degrees of freedom need to be solved. In our application, the finite element stiffness matrix is symmetric, positive definite and therefore the Preconditioned Conjugate Gradient (PCG) method is our method of choice. The PCG method is also well suited for parallel applications which are needed in practical applications.

Many finite element computations involve simulation of *inhomogenous* materials. These materials lead to large jumps in the entries of the stiffness matrix. We have shown in [3] that these jumps slow down the convergence of the PCG method and that by decoupling of those regions with a deflation technique a more robust PCG method can be constructed: the Deflated Preconditioned Conjugate Gradient (DPCG) method.

This paper extends the results we report on in [3]. The DPCG method uses deflation vectors that contain the rigid body modes of sets of elements with similar properties. We will derive a cheap and general applicable method to compute those rigid body modes. We also provide a mathematical justification of our approach. Finally, we will discuss numerical experiments on composite materials to validate our results.

2. Problem definition: composite materials

Until recently, because of the extremely long execution time, memory and storage space demands, the majority of FE simulations of composite materials were performed by means of homogenization techniques. Unfortunately these techniques do not provide an understanding of the actual interaction between the components of the material. Nevertheless, it is known that component interaction is the most critical factor in determining the overall mechanical response of the composite material.

In this paper, we consider asphalt concrete as an example of a composite material. It consists of a mixture of bitumen, aggregates and air voids. Obviously the difference between the stiffness of bitumen and the aggregates is significant, especially at higher temperatures. The stiffness of a material is determined by its Young's or E modulus and Poisson ratio.

We obtain accurate finite element meshes of the asphalt concrete materials by means of Computed Tomography (CT) X-ray scans and additional, specialized software tools like Simpleware ScanFE [6].

*Received by Copper Mountain student competition January 15, 2010.

†Delft University of Technology, Faculty of Civil Engineering, Department of Structural Mechanics, 2628CN Delft, the Netherlands (t.b.jonsthovel@tudelft.nl).

‡Delft University of Technology, Faculty of Information Technology and Systems, Department of Applied Mathematical Analysis, 2628CN Delft, the Netherlands (m.b.vangijzen@tudelft.nl, c.vuik@tudelft.nl).

2.1. **Stiffness matrix.** We use the computational framework described in [5] to simulate the response of a composite material that is subjected to external forces by means of small load steps. By using the FE method we obtain the corresponding stiffness matrix. Solving equation (1),

$$K\Delta u = \Delta f \tag{1}$$

is the most time consuming computation of the FE simulation. In this equation Δu represents the change of displacement of the nodes in the FE meshes and Δf the force unbalance in the system. The stiffness matrix K is symmetric positive definite for elastic, constrained systems, hence $\forall u \neq 0 : u^T K u > 0$ and all eigenvalues of K are positive. Within the context of mechanics, $\frac{1}{2}u^T K u$ is the strain energy stored within the system for displacement vector u, [1]. Energy is defined as a non-negative entity, hence the strain energy must be non-negative also.

3. On theory of DPCG

3.1. **Motivation of rigid body modes deflation.** We have shown in [3] that the number of iterations to convergence for preconditioned CG is highly dependent on the number of aggregates in a mixture as well as the ratio of the E moduli. Increasing the number of aggregates introduces correspondingly more clustered small eigenvalues in stiffness matrix K. The jumps in the E moduli are related to the size of the small eigenvalues. We know from [8] that the smallest eigenvalues correspond to the slow converging components of the solution.

When a matrix K_{unc} represents a rigid body, i.e. an unconstrained mechanical problem (with no essential boundary conditions) the strain energy equals zero for the rigid body displacements as the system remains undeformed and the matrix is positive semi-definite, $\forall u : u^T K_{unc} u \geq 0$. More specifically, the number of rigid body modes of any unconstrained volume, e.g., finite element, equals the number of zero-valued eigenvalues of its corresponding stiffness matrix. When a matrix has zero-valued eigenvalues the kernel $\mathcal{N}(A)$ is non-trivial. Moreover the basis vectors of the kernel of a stiffness matrix represent the principal directions of the rigid body modes. In general, two types of rigid body modes exist: translations and rotations. In three dimensions this implies six possible rigid body modes and hence six kernel vectors can be associated with the rigid body modes.

For any finite element computation we consider subsets of unconstrained elements as rigid bodies. Their corresponding (sub) stiffness matrices are assemblies of the element stiffness matrices. In the context of asphalt concrete the aggregates are subsets of elements, with their E modulus as a shared property, as well as the bitumen and the air voids.

In [3] we concluded that the number of aggregates times the number of rigid body modes per aggregate (6 in three dimensions) was equal to the number of smallest eigenvalues of stiffness matrix K. By using the deflation technique we augment the Krylov subspace with pre-computed rigid body modes of the aggregates and remove all corresponding small eigenvalues from the system. As a result the number of iterations of the Deflated Preconditioned Conjugated Gradient method is virtually not affected by jumps in material stiffness or by the number of aggregates.

3.2. **General deflation theory and preconditioned CG.** The deflation technique can be used in conjunction with ordinary preconditioning techniques such as diagonal scaling or Incomplete Cholesky factorization. This is a two-level approach, treating the smallest eigenvalues and largest eigenvalues with deflation and preconditioning respectively. By choosing a smart combination of deflation and preconditioning a more favorable spectrum is obtained, yielding a smaller condition number and less iterations.

For the description of deflation we split the solution of (1) into two parts [2]

$$u = \left(I - P^T\right) u + P^T u, \tag{2}$$

and let us define the projection P by,

$$P = I - KZ(Z^T KZ)^{-1} Z^T, \quad Z \in \mathbb{R}^{n \times m} \tag{3}$$

where Z is the deflation subspace, i.e. the space to be projected out of the system, and I is the identity matrix of appropriate size. We assume that $m \ll n$ and Z has rank m. Under this assumption $K_c \equiv Z^T KZ$ may be easily computed and factored and is symmetric positive definite. Hence,

$$\left(I - P^T\right) u = ZK_c^{-1} Z^T Ku = ZK_c^{-1} Z^T f \tag{4}$$

can be computed immediately. We only need to compute $P^T u$. Because KP^T is symmetric,

$$KP^T = PK, \tag{5}$$

we solve the deflated system,

$$PK\hat{u} = Pf \tag{6}$$

for $\hat{u}$ using the CG method and multiply the result by P^T. We should note that (6) is singular. However, the projected solution $P^T\hat{u}$ is unique, it has no components in the null space, $\mathcal{N}(PK) = \text{span}\{Z\}$. Moreover, from [4], [8] we learn that the null space of PK never enters the iteration process and the corresponding zero-eigenvalues do not influence the solution. To obtain a useful bound for the error of CG we define the effective condition number of a semi-definite matrix $C \in \mathbb{R}^{n \times n}$ with corank m to be the ratio of the largest and smallest positive eigenvalues,

$$\kappa_{\text{eff}}(C) = \frac{\lambda_n}{\lambda_{m+1}}. \tag{7}$$

We include Theorem 3.1 from [2] which implies that a bound on the condition number of PK can be obtained and leads to the choice of Z applied to the rigid body modes problems.

Theorem 3.1. *We assume a splitting $K = C + R$ such that C and R are symmetric positive semi-definite with $\mathcal{N}(C) = span\{Z\}$ the null space of C. Then*

$$\lambda_i(C) \leq \lambda_i(PK) \leq \lambda_i(C) + \lambda_{max}(PR). \tag{8}$$

Moreover, the effective condition number of PK is bounded by,

$$\kappa_{eff}(PK) \leq \frac{\lambda_n(K)}{\lambda_{m+1}(C)}. \tag{9}$$

We will use a symmetric preconditioner $M = LL^T$, e.g. diagonal scaling. We extend the result of Theorem 3.1 to,

$$\kappa_{\text{eff}}(L^{-1}PKL^{-T}) \leq \frac{\lambda_n(L^{-1}KL^{-T})}{\lambda_{m+1}(L^{-1}CL^{-T})}. \tag{10}$$

To illustrate the construction of the deflation vectors and a specific choice of Z we use the following experiment. Assume that we have a cube of bitumen containing one aggregate which is shown in Figure 1. The sub-domains Ω_1 and Ω_2 can be considered as bitumen and aggregates respectively. Clearly, without the constraints of the surrounding bitumen material, the aggregate of Ω_2 will act as a rigid body. With kernel deflation we aim to solve on both sub-domains separately. We separate sub-domain Ω_1 from sub-domain Ω_2 and apply new boundary conditions to the domains. We

assume that the aggregates that are not influenced by the boundary conditions of the whole domain act as rigid bodies, therefore we assume homogeneous Neumann boundary conditions. The bitumen will be restricted by the aggregates and we apply homogeneous Dirichlet boundary conditions.

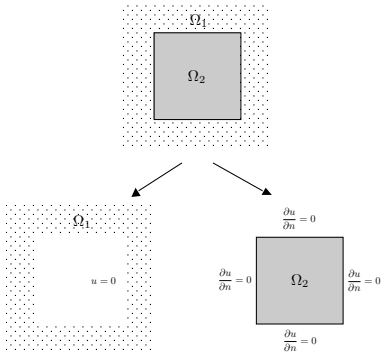

FIGURE 1. Principle of kernel deflation

The stiffness matrix is assembled from element stiffness matrices which come from the finite element formulation of the virtual work equation. Assume that we mesh the domain in Figure 1 with k elements. The mesh consists of 20 noded, cubic elements yielding element stiffness matrices $K_e \in \mathbb{R}^{60\times 60}$. We introduce the element operator $N_e \in \mathbb{R}^{60\times n}$ that maps a global vector to an element vector, $u_e = N_e u$. The stiffness matrix K is assembled by,

$$K = \sum_{e}^{m} N_e^T K_e N_e. \tag{11}$$

Assume that $K_b = \sum_{e\in\Omega_1} N_e^T K_e N_e$, $K_a = \sum_{e\in\Omega_2} N_e^T K_e N_e$ and $K_\Gamma = \sum_{e\in\Omega_1\cap\Omega_2} N_e^T K_e N_e$. We assume $K = C + R$ according to Theorem 3.1 where $C = K_b + K_a - K_\Gamma$ and $R = K_\Gamma$. Matrix C consists of two independent block matrices which correspond to the bitumen and aggregate domains. Matrix R consists of only those node contributions of elements from Ω_1 that lie on the intersection of domain Ω_1 and Ω_2. We should note that by the removal of the bitumen-aggregates boundary nodes from the bitumen sub-domain, Dirichlet and Neumann boundary conditions are automatically imposed on the bitumen and aggregate sub matrices in matrix C. The matrix C contains one singular sub matrix corresponding to the aggregate and one positive definite sub matrix corresponding to the bitumen. Moreover, because of the Dirichlet boundary conditions, the bitumen domain is statically determined and numerically well conditioned.

We apply Theorem 3.1 to $C = K_b + K_a - K_\Gamma$ and $R = K_\Gamma$. We have, $Z = \mathcal{N}(C) = \text{span}\{Z_a\}$ where $Z_a = \{z_a^1, ..., z_a^6\}$ with z_a^j the j-th base vector of the null space of K_b which correspond to all six rigid body modes of the aggregate. We must emphasize that by this choice of deflation subspace Z the rigid body modes are eliminated from the iterative solution process and removes the newly acquired Neumann boundary conditions from the aggregate sub-domains.

Extension of the previous experiment to an arbitrary number of aggregates and materials is straightforward. Section (3.4) provides two strategies on how to construct matrix Z.

3.3. **Computing rigid body modes (kernel) of a finite element.** We know from [1] that the rigid body modes of a finite element are spanned by the kernel base vectors of the corresponding element stiffness matrix. We will show a fast and cheap solution for the computation of the rigid

body modes. The same principle can be easily extended to sets of finite elements of arbitrary shape and order. We should note that the rigid body modes are only defined by the geometric properties of the element.

3.3.1. *3D rigid body motions.* In three dimensions a finite element has 6 rigid body motions; three translations and three rotations. For simplicity we consider a 4 noded tetrahedral element, however all derivations can be extended to N noded elements without loss of generality. The coordinate vector of the element is given by,

$$\left\{ \begin{array}{cccccccccccc} x_1 & y_1 & z_1 & x_2 & y_2 & z_2 & x_3 & y_3 & z_3 & x_4 & y_4 & z_4 \end{array} \right\}^T \tag{12}$$

A translation can be considered as a uniform displacement of every node in one principle direction. To obtain three orthogonal translations we choose the x,y and z direction respectively. The three translation vectors are given by,

$$\left\{ \begin{array}{cccccccccccc} 1 & 0 & 0 & 1 & 0 & 0 & 1 & 0 & 0 & 1 & 0 & 0 \end{array} \right\}^T \tag{13}$$

$$\left\{ \begin{array}{cccccccccccc} 0 & 1 & 0 & 0 & 1 & 0 & 0 & 1 & 0 & 0 & 1 & 0 \end{array} \right\}^T \tag{14}$$

$$\left\{ \begin{array}{cccccccccccc} 0 & 0 & 1 & 0 & 0 & 1 & 0 & 0 & 1 & 0 & 0 & 1 \end{array} \right\}^T \tag{15}$$

The rotations can be easily described using the spherical coordinate system,

$$x = r\cos(\theta)\sin(\phi), \tag{16}$$

$$y = r\sin(\theta)\sin(\phi), \tag{17}$$

$$z = r\cos(\phi) \tag{18}$$

where

$$r = \sqrt{x^2 + y^2 + z^2}, \tag{19}$$

$$\theta = \tan^{-1}\left(\frac{y}{x}\right), \tag{20}$$

$$\phi = \cos^{-1}\left(\frac{x}{r}\right) \tag{21}$$

and θ and ϕ as in Figure 2(a).

We derive a rotation $d\theta$ in the x, y-plane, hence $d\phi = 0$ and $dr = 0$. The x-y, x-z and y-z planes contain unique rotations. The corresponding vectors can be found by swapping axis. For an arbitrary point in space which has spherical coordinates (r, θ, ϕ) a change $d\theta$ in the x, y-plane yields a displacement in cartesian coordinates of,

$$dx = -r\sin(\theta)\sin(\phi)d\theta, \tag{22}$$

$$dy = r\cos(\theta)\sin(\phi)d\theta, \tag{23}$$

$$dz = 0. \tag{24}$$

Figure 2(b) shows the rotation for one element with respect to the origin over angle $d\theta$. By using above expressions we obtain all three rotation vectors, given by Table 1.

3.3.2. *Construction of the deflation matrix Z.* We compute the null space of each element matrix by the method explained in the previous section. We consider a structure that consists of regions. We define the region R_p as a collection of elements that share a certain property and are neighbors. The rigid body modes of a collection of elements is equal to the assembly of the rigid body modes of the individual elements taking into account the multiplicity of those degrees of freedom that lie in multiple neighboring elements. In the case of asphaltic materials we choose the element stiffness

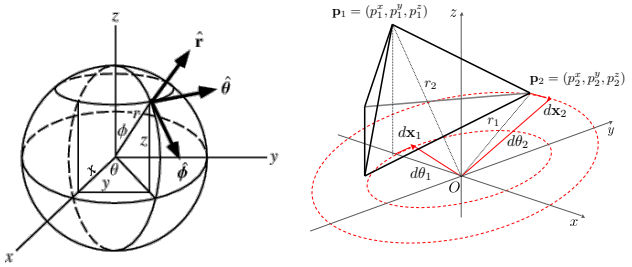

(a) (b)

FIGURE 2. 2(a) spherical coordinates, 2(b) rotation around origin of tetrahedral element in x, y-plane

TABLE 1. Rotations

(a) **rotation x-y plane**

$$\theta_j = \tan^{-1}\left(\frac{y_j}{x_j}\right) \phi_j = \cos^{-1}\left(\frac{z_j}{r_j}\right) \quad \left\{ \begin{array}{c} -r_1 \sin(\theta_1)\sin(\phi_1) \\ r_1 \cos(\theta_1)\sin(\phi_1) \\ 0 \\ -r_2 \sin(\theta_2)\sin(\phi_2) \\ r_2 \cos(\theta_2)\sin(\phi_2) \\ 0 \\ -r_3 \sin(\theta_3)\sin(\phi_3) \\ r_3 \cos(\theta_3)\sin(\phi_3) \\ 0 \\ -r_4 \sin(\theta_4)\sin(\phi_4) \\ r_4 \cos(\theta_4)\sin(\phi_4) \\ 0 \end{array} \right\},$$

(b) **rotation y-z plane**

$$\theta_j = \tan^{-1}\left(\frac{z_j}{x_j}\right) \phi_j = \cos^{-1}\left(\frac{y_j}{r_j}\right) \quad \left\{ \begin{array}{c} -r_1 \sin(\theta_1)\sin(\phi_1) \\ 0 \\ r_1 \cos(\theta_1)\sin(\phi_1) \\ -r_2 \sin(\theta_2)\sin(\phi_2) \\ 0 \\ r_2 \cos(\theta_2)\sin(\phi_2) \\ -r_3 \sin(\theta_3)\sin(\phi_3) \\ 0 \\ r_3 \cos(\theta_3)\sin(\phi_3) \\ -r_4 \sin(\theta_4)\sin(\phi_4) \\ 0 \\ r_4 \cos(\theta_4)\sin(\phi_4) \end{array} \right\},$$

(c) **rotation x-z plane**

$$\theta_j = \tan^{-1}\left(\frac{z_j}{y_j}\right) \phi_j = \cos^{-1}\left(\frac{x_j}{r_j}\right) \quad \left\{ \begin{array}{c} 0 \\ r_1 \cos(\theta_1)\sin(\phi_1) \\ -r_1 \sin(\theta_1)\sin(\phi_1) \\ 0 \\ r_2 \cos(\theta_2)\sin(\phi_2) \\ -r_2 \sin(\theta_2)\sin(\phi_2) \\ 0 \\ r_3 \cos(\theta_3)\sin(\phi_3) \\ -r_3 \sin(\theta_3)\sin(\phi_3) \\ 0 \\ r_4 \cos(\theta_4)\sin(\phi_4) \\ -r_4 \sin(\theta_4)\sin(\phi_4) \end{array} \right\}.$$

as the property for discrimination between elements. Elements with corresponding stiffness make up one independent region. We can think of stones, bitumen and air voids. We should note that we can have more than three regions in this example, because we can have multiple stones, separated by bitumen or air voids. Each element in 3D has 6 rigid body motions, hence the total number

of deflation vectors $L = N_R \times 6$ where $N_R = \sum_{p=1}^{P} N_{R_p}$, and N_{R_p} is the number of regions per property p.

For each region R_p and $\forall e \in R_p$ we construct a deflation matrix $Z^p = \sum_{e=1}^{E} N_e^T W_e^p Z_e^p$, where Z^p is the deflation matrix and has dimension $N \times N_{R_p}$, E is the number of elements in Ω, N_e is the FE assembly operator of element e and has dimension $k \times N$, W_e^p is the diagonal scaling matrix of element e and has dimension $k \times k$ and Z_e^p is the deflation matrix of element e and has dimension $k \times k$. The diagonal scaling matrix W_e^p contains ones on the main diagonal for corresponding degrees of freedom that have no overlap with neighboring elements and 1 over the number of elements the degree of freedom is contained in for this region p. By doing so we ensure that the multiplicty of shared nodes in neighboring elements is taken into account.

The deflation matrix $Z = [Z_1, ..., Z_{N_R}]$ has dimension $N \times L$. The assembled deflation matrix Z is sparse because rigid body modes of disjoint regions do not overlap, hence it can be stored in an efficient way.

3.4. **Deflation strategies.** Different choices of properties imply different regions, hence we can think of different deflation strategies. For more complex finite element meshes, as in the numerical examples of Section (4), it is non-trivial how to choose the regions.

We introduce two different strategies. Both strategies rely on discrimination between elements based on material stiffness. The main purpose of introducing two strategies is to illustrate the necessity of a sound mathematical reason behind the deflation strategy. Deflation does not work for an arbitrary selection of deflation vectors.

3.4.1. *Strategy I: recursive decoupling.* The main idea behind the proof of Section (3.2) is a decoupling of the aggregate region from the surrounding bitumen region by effectively imposing Dirichlet boundary conditions on the bitumen and Neumann boundary conditions on the aggregates. When the complexity of the structure increases, e.g. aggregates surrounded by bitumen and air voids, we can use a recursive decoupling. Figure 3 shows a more complex structure. The dark gray areas are aggregates, the dotted areas are bitumen and the striped areas represent air voids. Clearly, all materials are connected. We use the argument of Section (3.2) to motivate the recursive decoupling deflation strategy. We start by considering the whole structure as one rigid body. This means that for the splitting of $K = C + R$, $C = K$ and $R = 0$. The next step is imposing Dirichlet boundary conditions on the boundaries between the air voids and the combined areas of bitumen and aggregates and Neumann boundary conditions on the latter, yielding $C = K_{bit,agg} + \tilde{K}_{air} - K_{\Gamma,air}$ and $R = K_{\Gamma,air}$. $\tilde{K}_{air}$ represents the assembled stiffness matrix of the air void elements without the boundary nodes which are contained in $K_{\Gamma,air}$. The last decoupling is between the aggregates and the areas with bitumen and air voids. We impose Dirichlet boundary conditions on the bitumen and air voids and Neumann boundary conditions on the aggregates, yielding $C = K_{bit} + \tilde{K}_{bit,air} - K_{\Gamma,bit,air}$ and $R = K_{\Gamma,bit,air}$. $\tilde{K}_{bit,air}$ represents the assembled stiffness matrix of the air void and bitumen elements without the boundary nodes which are contained in $K_{\Gamma,bit,air}$.

3.4.2. *Strategy II: overlapping regions.* Strategy II is based on discrimination between elements on basis of material stiffness. However, when two regions have overlap at region boundary nodes, we exclude those boundary nodes that correspond to the region which has the lowest stiffness. This strategy is based on the ideas proposed in [3] and [9].

3.5. **DPCG algorithm.** The DPCG method [7] is given by Algorithm 1.

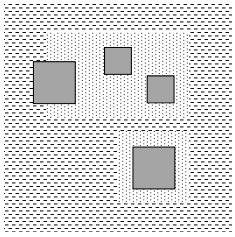

FIGURE 3. increased complexity in structure of mixture of materials

Algorithm 1 Deflated preconditioned CG solving $K\mathbf{u} = \mathbf{f}$

Select $\mathbf{u}_0$. Compute $\mathbf{r}_0 = (\mathbf{f} - K\mathbf{u}_0)$, set $\hat{\mathbf{r}}_0 = P\mathbf{r}_0$ and $\mathbf{p}_0 = \hat{\mathbf{r}}_0$
Solve $M\mathbf{y}_0 = \hat{\mathbf{r}}_0$ and set $\mathbf{p}_0 = \mathbf{y}_0$
for $j = 0, 1, \ldots$ until convergence **do**
  $\hat{\mathbf{w}}_j = PK\mathbf{p}_j$
  $\alpha_j = \frac{\left(\hat{\mathbf{r}}_j, \mathbf{y}_j\right)}{\left(\hat{\mathbf{w}}_j, \mathbf{p}_j\right)}$
  $\hat{\mathbf{u}}_{j+1} = \hat{\mathbf{u}}_j + \alpha_j \mathbf{p}_j$
  $\hat{\mathbf{r}}_{j+1} = \hat{\mathbf{r}}_j - \alpha_j \hat{\mathbf{w}}_j$
  Solve $M\mathbf{y}_{j+1} = \hat{\mathbf{r}}_{j+1}$
  $\beta_j = \frac{\left(\hat{\mathbf{r}}_{j+1}, \mathbf{y}_{j+1}\right)}{\left(\hat{\mathbf{r}}_j, \mathbf{y}_j\right)}$
  $\mathbf{p}_{j+1} = \mathbf{y}_{j+1} + \beta_j \mathbf{p}_j$
end for
$\mathbf{u} = ZK_c^{-1}Z^T\mathbf{f} + P^T\hat{\mathbf{u}}_{j+1}$

4. NUMERICAL EXPERIMENT

The case given by Figure 4 is a small asphalt concrete fragment from a real life CT scan. Multiple aggregates are embedded in a layer of bitumen and air voids. We compare DPCG and PCG in combination with diagonal scaling. The case involves a mixture of materials that is subjected to an external force applied to the upper boundary of the volume. Zero displacement boundary conditions are imposed on the base of the volume, this is homogenous Dirichlet boundary conditions to all degrees of freedom in the x, z-plane for $y = 0$. We should note that the case resembles the uniaxial compression test, which is a standard laboratory test. We observe the convergence behavior of DPCG, with deflation strategies I and II, and PCG for variations in the E modulus of the bitumen and aggregates as given by Table 2 (a). We compare a standard choice of parameters [5] with increased stiffness of the aggregates (a) and bitumen (b).

TABLE 2

(a) E modulus materials

	aggregate	bitumen	air voids
standard	70000	5000	100
(a)	**700000**	5000	100
(b)	70000	**50000**	100

(b) color codes numerical results

standard	E modulus (a) or (b)
pcg, ●	pcg, ●
dpcg, strategy I, ●	dpcg, strategy I, ●
dpcg, strategy II, ●	dpcg, strategy II, ●

Figure 5 shows the regions that belong to deflation strategy I. With 78 deflation vectors (13 regions), strategy II is slightly more expensive than strategy I which uses 60 deflation vectors (10 regions). The numerical results of Figure 6 show that DPCG with deflation strategy I is almost

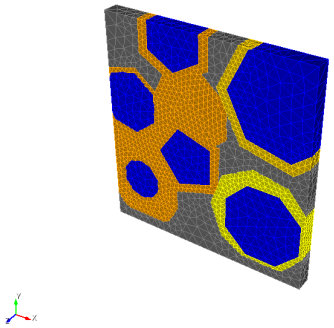

FIGURE 4. slice of mixture of materials from CT scan: unstructured mesh contains 32883 nodes and 98340 degrees of freedom

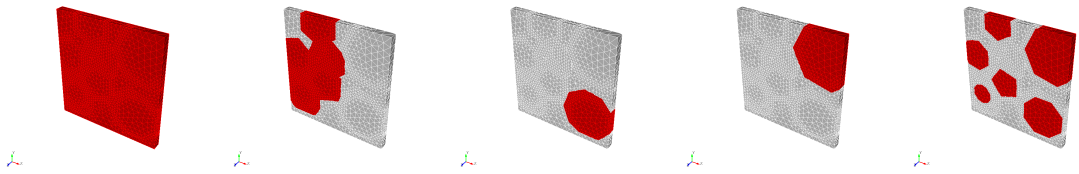

(a) (b) (c) (d) (e)

FIGURE 5. deflation strategy I: the red areas are sets of elements that form one region. (a) all elements, (b,c,d) all elements that have bitumen or aggregate stiffness, (e) all elements that have aggregate stiffness

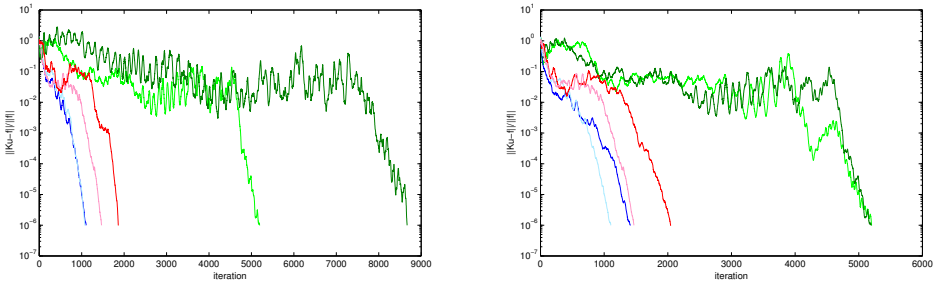

(a) (b)

FIGURE 6. numerical results: different E moduli, see Table 2 (b)

invariant under change of the E modulus of both the aggregates and the bitumen. The convergence of PCG remains almost invariant under increase of the E modulus of the bitumen. In case of strategy II, we can see from the plateau in the convergence path that small eigenvalues corresponding to

large jumps still exist in the deflated system, clearly not all regions have been decoupled. In table 3 we observe that the amount of extra work is negligible compared to the gain in performance and stability. When we compare PCG to DPCG with strategy I (DPCG I) for the standard case, we gain a reduction in iterations of factor 4.7 and a reduction in CPU wall time of factor 3.3. This is implies that DPCG I only requires a factor of 1.42 more work per iteration. This number becomes even more favorable for DPCG I (1.29 for (a), 1.32 for (b)) when the gap in iterations between PCG and DPCG increases.

TABLE 3. CPU wall time(s) PCG and DPCG (parallel implementation, MPI, 8 CPUs Intel Xeon E5450 running at 3.00GHz)

	PCG		DPCG I		DPCG II	
	iter	cpu (s)	iter	cpu(s)	iter	cpu(s)
standard	5195	30	1107	9	1469	10
(a)	8670	50	1077	8	1864	11
(b)	5201	28	1414	10	2046	13

5. Conclusion

We described a simple general applicable way on how to choose deflation vectors by using the rigid body modes of subsets of elements. By combining the deflation technique and the computation of the exact rigid body modes of the components the robust deflated preconditioned gradient method (DPCG) is obtained. The DPCG method is insensitive to large jumps in the E modulus of materials. The amount of extra work needed for DPCG is negligible.

References

[1] K. J. Bathe. *Finite Element Procedures*. Prentice Hall, 2 revised ed edition, June 1995.
[2] J. Frank and C. Vuik. On the construction of deflation-based preconditioners. *SIAM J. Sci. Comput.*, 23(2):442–462, 2001.
[3] T.B. Jönsthövel, M.B. van Gijzen, C.Vuik, C. Kasbergen, and A. Scarpas. Preconditioned conjugate gradient method enhanced by deflation of rigid body modes applied to composite materials. *Computer Modeling in Engineering and Sciences*, 47:97–118, 2009.
[4] E. F. Kaasschieter. Preconditioned conjugate gradients for solving singular systems. *J. Comput. Appl. Math.*, 24(1-2):265–275, 1988.
[5] A. Scarpas. *Mechanics based computational platform for pavement engineering*. PhD Thesis TU Delft, 2004.
[6] Simpleware. http://www.simpleware.com, 2009.
[7] J.M. Tang. *Two-Level Preconditioned Conjugate Gradient Methods with Applications to Bubbly Flow Problems*. PhD Thesis TU Delft, 2008.
[8] A. Van der Sluis and H.A. Van der Vorst. The rate of convergence of conjugate gradients. *Numer. Math.*, 48(5):543–560, 1986.
[9] F. Vermolen, C. Vuik, and A. Segal. Deflation in preconditioned conjugate gradient methods for finite element problems. In M. Křižek, P. Neittaanmäki, R. Glowinski, and S. Korotov, editors, *Conjugate Gradient and Finite Element Methods*, pages 103–129. Springer, Berlin, 2004.